2011 IEEE/RSJ International Conference on
Intelligent Robots and Systems
September 25-30, 2011. San Francisco, CA, USA

Beyond Visual Range Obstacle Avoidance and Infrastructure Inspection by an Autonomous Helicopter

Torsten Merz and Farid Kendoul

Abstract— **This paper demonstrates the feasibility of accomplishing real-world inspection tasks beyond visual range with an autonomous helicopter using simple but effective methods. We propose a LIDAR-based perception and guidance system that enables a helicopter to perform obstacle detection and avoidance, terrain following, and close-range inspection. The system has been implemented on board the CSIRO unmanned helicopter and flight tested in a number of different mission scenarios in unknown environments. We have successfully completed 37 missions and recorded more than 14 hours of autonomous flight time. Missions beyond visual range were executed without a backup pilot. The system has achieved a high success rate and has proven to be dependable.**

I. INTRODUCTION

There is a significant increase in the deployment of Unmanned Aircraft Systems (UAS) for a variety of military and civilian applications. However, operations are often limited to flights at medium or high altitude or flights under close human supervision. On the other hand, there is a high demand for low-altitude flights in search and rescue, surveillance and reconnaissance, and infrastructure inspection. Such flights present challenges on the maneuverability of an aircraft, its capability to navigate among obstacles, and its operation beyond visual range (BVR).

In this paper, we present an autonomous unmanned helicopter system (see Figure 1) capable of performing inspection tasks in unknown environments. The methods we propose are designed to work with a large variety of rotorcraft. We focused on larger helicopters as they are most likely to be chosen for long-distance BVR flights. The CSIRO unmanned helicopter is large enough to reveal characteristics and constraints of larger rotorcraft which one might not consider using smaller platforms.

Our system enables BVR operations close to obstacles at low altitude without the need for a backup pilot. Three main capabilities have been identified as being essential for autonomous operations: (1) BVR waypoint navigation flight; (2) ground detection and terrain following; and (3) obstacle detection and avoidance. In the next paragraphs, we briefly present related work and state of the art in these technologies.

GPS-based waypoint navigation for unmanned rotorcraft is becoming a mature technology and most research groups have integrated this capability in their platforms. However, we are not aware of any system developed by an academic research group enabling BVR operations in unknown environments as specified above.

T. Merz and F. Kendoul are with the Australian Research Centre for Aerospace Automation (ARCAA), 22-24 Boronia Road, Eagle Farm, 4009, Queensland and CSIRO ICT Centre, PO Box 883, Kenmore, Queensland, Australia. Email: torsten.merz@csiro.au, farid.kendoul@csiro.au

Fig. 1. The CSIRO autonomous helicopter with inspection payload.

Although ground detection and terrain following are important capabilities for rotorcraft flights at low altitudes, only few works address this problem. Bio-inspired optic flow methods have been investigated for terrain following and demonstrated on small indoor rotorcraft such as quadrotors [1], a 100-gram tethered rotorcraft [2], and a larger outdoor unmanned helicopter [3].

The sensing technologies commonly used on unmanned rotorcraft for perception in general and obstacle avoidance in particular, are computer vision (passive sensing) and LIDAR systems (active systems). A variety of approaches to the obstacle avoidance problem on board an aircraft exists. They can be classified into two main categories: SMAP-based approaches and SMAP-less techniques. In the *SMAP* (*Simultaneous Mapping And Planning*) framework, mapping and planning are jointly performed to build a map of the environment which is then used for path planning. SMAP-less obstacle avoidance strategies are generally reactive without the need for a map or a path planning algorithm.

In literature, most SMAP-less approaches are vision-based, where obstacles are detected and avoided using optic flow [4–8] or a priori knowledge of some characteristics of the obstacle such as color and shape [9]. SMAP-less techniques are attractive because of their simplicity and real-time capabilities. However, no convincing results have been obtained yet that demonstrate their effectiveness for achieving real-world applications in natural unknown environments.

On the other hand, SMAP-based approaches have been proven to be an effective way for dealing with obstacles in unknown environments. However, they are computation-

978-1-61284-456-5/11/$26.00 ©2011 Crown

ally expensive, especially those based on computer vision. Although many papers have been published on computer vision for rotorcraft obstacle avoidance, very few systems have been implemented on an actual aircraft and modest experimental results have been reported in the literature [10, 11] . Major significant achievements in 3D perception and obstacle avoidance by unmanned rotorcraft have been obtained using LIDAR systems and a SMAP-based approach. To our knowledge, the most successful implementations on rotorcraft are the ones by CMU [12] (custom 3D LIDAR from Fibertek Inc. and potential functions based global and local 3D path planners), US Army/NASA [13, 14] (spinning SICK LIDAR and 3D A* planning algorithm), Berkeley University [15] (2D SICK LIDAR and model predictive controller for path planning and flight control), and MIT [16] (indoor navigation using a 2D Hokoyu LIDAR and planning algorithm).

In the framework of the *Smart Skies* project [17], the CSIRO UAS team has been engaged in two main areas of research: dependable autonomous flight beyond visual range and low-altitude obstacle field navigation. The main contribution of this paper is the development of a LIDAR-based SMAP-less approach that demonstrates the feasibility of accomplishing BVR obstacle avoidance and infrastructure inspection tasks by only using a vertically mounted 2D lightweight LIDAR and reactive behaviors (no planning) in a goal-oriented navigation framework. Rather than using expensive and heavy 3D LIDARs or spinning/sweeping mechanisms for 2D LIDARs, our system uses a COTS 2D LIDAR in combination with two special helicopter flight modes to address the problem of 3D perception. Moving the helicopter to extend the field of view of a 2D LIDAR reduces weight, power, and the risk of failure of a spinning/sweeping mechanism.

II. SPECIFICATION OF INSPECTION TASKS

In this work, we consider two types of inspection tasks[1]: inspections of ground objects and inspections of vertical structures. The task goals for for the helicopter are:

Task 1 Delivery[2] of aerial photos of specified locations with at least one usable[3] photo per location.

Task 2 Delivery of at least one usable photo of a side of a vertical structure.

In addition, the goal is not to damage the aircraft or objects in the environment. Both tasks are required to be accomplished autonomously[4] in unknown environments[5].

For task 1, image-capturing positions (*inspection points*) are specified by a list of geographic coordinates (e.g. from satellite images) and heights above ground. For task 2, the user provides: (1) the position of the vertical structure (*target point*); (2) an *approach point*; and (3) a height above ground. The helicopter approaches the structure from the approach point and stops at a close but safe distance at the given height for taking images (inspection point). The horizontal positions of the target and approach points are defined in geographic coordinates.

A task is decomposed into three stages: (1) the flight from a *start point* to the inspection area; (2) the flight in the inspection area; and (3) the flight from the inspection area to a given *end point*. The helicopter hovers at the start and end point (autonomous take off and landing is not part of this work). The user can define additional waypoints for the flight to and from the inspection area. Waypoints are defined in flight plans which are uploaded to the helicopter through a wireless data link. The horizontal positions of waypoints are defined in geographic coordinates and their height is relative to the take off point.

The inspection area is envisaged to be within a height-limited segregated airspace, whereas the start and end points are envisaged to be in common airspace. The segregated airspace is entered from above at a user defined *descent point*. For flights in common airspace, the helicopter interacts with an air traffic control system to ensure separation from other air traffic. In this work, the helicopter interacts with the *Automated Dynamic Airspace Controller* (ADAC) system which has been developed by our project partner *Boeing Research and Technology USA* in the Smart Skies project [17]. Before commencing a flight in common airspace, the helicopter sends a flight plan to the ADAC. During flight plan execution, the helicopter transmits state estimates to the system. In case of a conflict with other air traffic, the ADAC sends flight plan alterations to aircraft in the area. The communication is realized through mobile networks and the Internet.

The following assumptions are made about obstacles in the inspection area: (1) there are no obstacles between the approach point and the structure; (2) there are no obstacles in the close vicinity of the descent point; and (3) there is a safe path to the inspection points. If one of these assumptions is violated the helicopter system may immediately leave the inspection area and fly to the end point.

The following *critical* assumptions are made: There are possibly other aircraft but no static obstacles in the area of operations in common airspace. This assumption is realistic as flights in common airspace are usually conducted at higher altitudes. Instructions on how to avoid other aircraft must be provided by an air traffic control system. We assume obstacles in the inspection area are: (1) static; (2) large enough for the LIDAR to detect; and (3) not in a cylinder of 10m radius 5m above the helicopter. Positions and velocities are provided by GPS. The horizontal position error of the GPS is assumed to be less than 5m and the horizontal velocity error less than 0.5m/s. Due to power limitations of our helicopter, the wind must be less than 10m/s and downdrafts less than 2.0m/s . Finally, we assume there is no rain, fog, snow, or dust. A violation of a critical assumption could result in a failure.

An inspection mission is an inspection task performed in a specific environment. A mission is *successful* if the helicopter autonomously achieves the goal of an inspection

[1]This work addresses only the data collection part of an inspection.

[2]Photos are available for download at a specified location.

[3]A photo which contains useful information for an inspection.

[4]Task accomplishment without pilot or interaction with external systems other than GPS or an air traffic control system.

[5]No information about terrain elevation and static obstacles is provided.

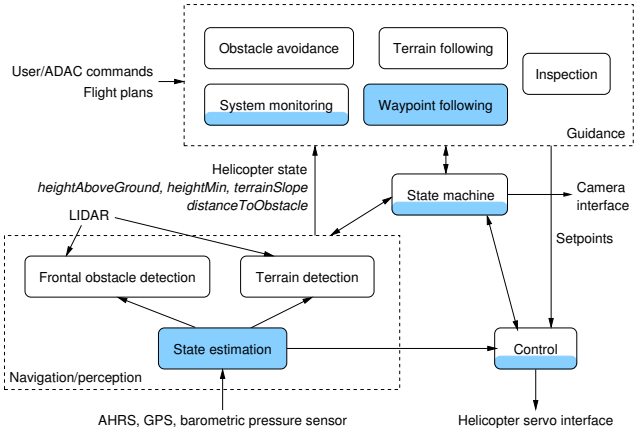

Fig. 2. Architecture of the BVR infrastructure inspection system.

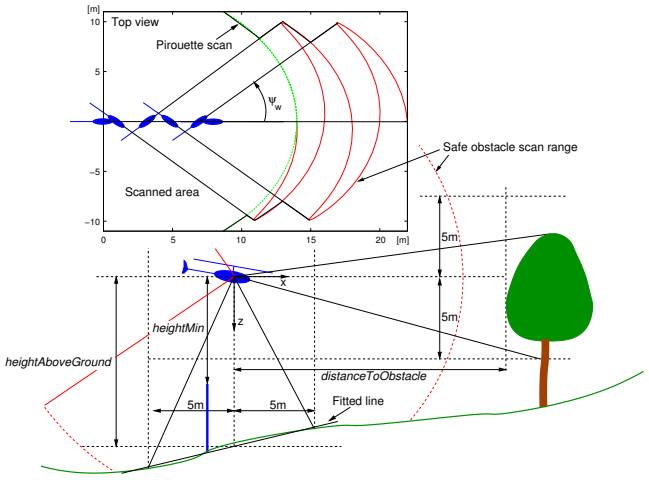

Fig. 3. Illustration of LIDAR-based terrain and obstacle detection methods.

task. A mission *fails* if: (1) a backup pilot takes over control; or (2) the helicopter does not reach the end point; or (3) the helicopter is no longer suitable for safe flight. According to the above definition, an unsuccessful mission is not necessarily a failed mission. For instance, if for safety reasons the helicopter aborts a mission, we do not consider the mission to be a failure.

III. SYSTEM COMPONENTS AND METHODS

During the last three years, we have devoted much effort to the development of a dependable autonomous helicopter base system with BVR waypoint navigation capability. The BVR inspection capability is built on top of the base system by extending the guidance system and by adding flight modes and perception functions. The base system is capable of executing stage 1 and 3 of an inspection task (see Section II). This paper focuses on the extensions required for stage 2, a detailed description of the base system will be published separately.

Figure 2 shows a simplified block diagram of the architecture of the BVR infrastructure inspection system. Components of the base system are highlighted in blue. The basic flight modes are hover, yaw, vertical climb/descend, and horizontal straight line path following. They are based on decoupled SISO PID controllers with a nested control loop scheme using helicopter state estimates. For the inspection tasks we added a *waggle cruise* and a *pirouette descent* flight mode which are based on the basic flight modes.

The execution of individual tasks is controlled by a state machine. A system monitor analyzes the helicopter state estimates and provides the state machine with information for transition making.

A. Perception

3D perception is a crucial component for low-altitude flights in unknown environments. Our solution consists of a vertically mounted 2D LIDAR[6] and two special flight modes.

[6]The LIDAR is mounted together with the AHRS of the navigation system on a common structure. The proposed methods tolerate small alignment errors.

The *pirouette descent*[7] mode creates a spinning LIDAR with a cylindrical field of view by rotating the helicopter around its yaw axis while descending vertically. The *waggle cruise*[8] flight mode performs a horizontal sweep while flying forward, allowing to scan a corridor-shaped space. This is an alternative to the *stop-and-scan* approach often used for ground robots which is inefficient in our case as the safe range of the LIDAR and the size of the desired safety corridor (12m frontal and $\pm$10m lateral) are nearly the same. The safe range is the maximum range for the LIDAR to detect an obstacle with high probability in a typical outdoor environment. For our LIDAR it is 18m for terrain and 14m for frontal obstacles.

For efficiency requirements, the proposed perception method does not process all LIDAR data, but rather selects two sections of the scan that contain useful information about the terrain and frontal obstacles as illustrated in Figure 3.

1) Terrain detection: The method developed for terrain detection uses state estimates and a section of the LIDAR scan to compute the terrain slope below the helicopter and the distance between the helicopter and the terrain. The data synchronization is done as follows. A real-time task in the navigation computer which is synchronized with the AHRS[9] generates state estimates with 100Hz update rate. An independent real-time task matches range data with the last state estimate at the time a scan sync pulse is received from the LIDAR.

Height estimation is based on a line-fitting algorithm which is applied to the LIDAR returns of $\pm$5m terrain below the helicopter after compensating for roll and pitch angles (see Figure 3). The two estimated parameters of the line are the terrain slope and the helicopter height above ground. In addition to these two parameters, the algorithm also computes the minimum height (*heightMin*) that has been

[7]The yaw controller is tracking a linear reference trajectory with 45°/s angular rate. The vertical speed is 1m/s.

[8]The yaw controller is tracking a sinusoidal reference trajectory with $\psi_w = 45°$ amplitude and 4s waggle period time. The path following controller independently controls the distance to the path and the path speed.

[9]The AHRS includes a magnetometer for heading estimation.

sensed underneath the helicopter. The minimum height is used to detect small vertical obstacles that may be filtered by the line-fitting algorithm.

2) Obstacle and target detection: The method is similar to the one used for terrain detection since it also finds the minimum distance in an attitude compensated section of a LIDAR scan (see Figure 3). The minimum distance corresponds to the closest frontal obstacle. To detect small obstacles (e.g. wires) sensed with a single LIDAR beam, the method does not include any fitting or filtering algorithms. This is also motivated by the fact that false positives are very rare except in the presence of rain, dust, etc. At each sampling time, the obstacle detection method outputs the distance to the closest obstacle (*distanceToObstacle*) in front of the helicopter along the x-axis. During waggle cruise, the helicopter scans the environment in the horizontal plane as illustrated in Figure 3 (top view).

Although these perception methods are rudimentary and simple, they turned out to be very effective in practice. Indeed, the helicopter performed more than 11 hours of autonomous obstacle avoidance and terrain following in different environments without any problems related to terrain and obstacle detection.

B. Descent and terrain following

We implemented a LIDAR-based terrain following flight mode for approaching inspection points at low altitude. The helicopter switches from pressure-based to LIDAR-based height control at the descent point (see Section II). It descends based on barometric height estimates until the height above ground is less than the vertical safe LIDAR range (see Section III-A). The helicopter stops, switches from pressure to LIDAR-based height control and continues descending to the desired height above ground. During the vertical descent the helicopter continuously rotates around its yaw axis for obstacle detection (pirouette descent). While flying to inspection points, the system regulates the height above ground to the desired height, resulting in a LIDAR-based terrain following system.

A safety monitoring module has been added to the system which aborts an inspection task and commands the helicopter to climb to safe altitude if the *heightMin* value is less than a specified threshold or the LIDAR no longer detects the terrain. The former is usually caused by small vertical obstacles below the helicopter or a significant positive terrain discontinuity. The latter can be due to a LIDAR failure or a significant negative terrain discontinuity.

In most flight experiments presented in Section IV-C, the desired height above ground was set to 10m or 5m, and the *heightMin* threshold was set to half of that value. In order to reduce the number of aborted missions due to the *heightMin* threshold, a simple strategy was implemented to monitor the *heightMin* value and to command a height offset when the value approaches the threshold. This simple strategy has been proven to deal with terrain discontinuities such as small trees, fences, roofs, vehicles, etc.

C. Obstacle avoidance

The obstacle avoidance system is based on reactive behaviors combined with a goal-oriented navigation approach. The latter is required as the task is not only to avoid an obstacle but also to arrive at a given waypoint. Similar to the terrain following approach, we included a safety monitoring module which aborts an inspection task and commands the helicopter to climb to safe altitude if the *distanceToObstacle* value is less than a specified threshold (5m).

In the following, we present two different avoidance strategies for a flight from one waypoint (*origin point*) to another waypoint (*destination point*). Both strategies have been implemented on the helicopter and flight tested in various scenarios.

Strategy 1: The main steps of this strategy are:

1) The helicopter flies in waggle cruise mode towards the destination point until it reaches the point or detects an obstacle ($distanceToObstacle < 15$m). If it reaches the point, the algorithm terminates.
2) The helicopter stops and generates an avoidance waypoint. The waypoint is defined in polar coordinates[10] with respect to the current helicopter position and ground track.
3) The helicopter flies towards the avoidance waypoint in waggle cruise mode until it reaches the point or detects an obstacle. If it reaches the avoidance waypoint, it flies towards the destination point as described in step 1, otherwise steps 2 and 3 are repeated.

The initial avoidance direction (right or left) must be defined before take off. If the helicopter does not reach the destination point after a number of attempts it will return to the origin point and try to avoid the obstacle from the other direction.

Strategy 2: Experimental flights with strategy 1 have shown that the helicopter arrives at destination points in many different scenarios within its maximum available safe flight time (see Section IV). However, this strategy may suffer from the local minima problem in environments with concave shaped obstacle configurations ("U" shape). Therefore, we developed a more complex reactive avoidance strategy that is based on the "wall following" principle. As illustrated in Figure 4, the basic idea behind this strategy is to "track" the obstacle until the helicopter is close to the original path. We also added a function for deciding the initial avoidance direction.

The main steps of strategy 2 are:

1) The helicopter flies in waggle cruise mode towards the destination point until it reaches the point or detects an obstacle in the safety corridor (see Section III-A). If it reaches the point, the algorithm terminates.
2) The helicopter stops and scans the environment by yawing $\pm 60^\circ$ with respect to the last ground track. It chooses the avoidance direction (right or left) based on the detected free space.

[10] $avoidanceAngle = \pm 90^\circ$, $avoidanceWpDistance = 12$m

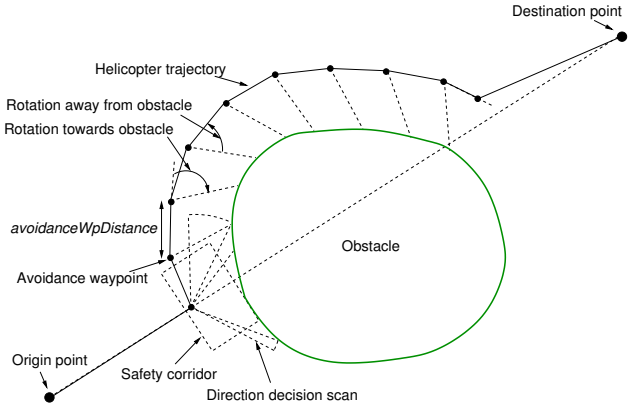

Fig. 4. Second strategy for obstacle avoidance.

3) The helicopter generates an avoidance waypoint as follows:
   - It rotates towards the obstacle with a maximum angle of 120° until it detects the obstacle or reaches the maximum angle.
   - If it detects the obstacle, it rotates away from the obstacle with a maximum angle of 360° until it has enough clearance from the obstacle (60° section with *distanceToObstacle* > 15m). If the helicopter reaches the maximum angle, the algorithm terminates with an error (helicopter trapped). The avoidance waypoint is defined as the point which is at a distance of *avoidanceWpDistance* = 12m in front of the helicopter.
   - If it does not detect the obstacle, it continues the flight to the destination point as described in step 1.
4) The helicopter flies towards the avoidance waypoint in waggle cruise mode until it reaches the point or detects and obstacle in the safety corridor.
5) Steps 3 and 4 are repeated until the system is commanded to abort the wall-following and to fly to the destination point as described in step 1. The wall-following is aborted in the following situations:
   - The helicopter is close to the direct path from origin to destination point and there is progress, i.e. the helicopter gets closer to the destination point.
   - The helicopter has not succeeded to reach the destination point after a certain number of attempts. If progress was made during wall following, the origin point will be set to the current position. Otherwise the next obstacle will be avoided from the other direction.
   - The helicopter leaves a user defined corridor along the direct path from origin to destination point. The next obstacle will be avoided from the other direction.

D. Image capturing

For task 1, the inspection camera is mounted vertically. At each inspection point, the helicopter changes its height to the desired image-capturing height and takes images while hovering. For task 2, the camera is mounted horizontally and aligned with the fuselage. Images of vertical structures are taken as follows:

1) The helicopter flies from the approach point towards the target point in waggle cruise mode until it detects an obstacle or reaches the target point. If it reaches the point, the algorithm terminates with an error (no target).
2) The target is identified if the helicopter hovers within a specified range to the target point (18m). If it is outside that range the algorithm terminates with an error.
3) The helicopter changes its height to the desired image-capturing height and takes images while yawing ±30° with respect to the last ground track.

IV. FLIGHT TESTS AND RESULTS

The BVR infrastructure inspection system has undergone an extensive program of flight tests using the CSIRO unmanned helicopter. The objective of these flight tests was to evaluate the performance of the complete system in realistic mission scenarios under a wide range of conditions, but also to identify its limitations and weaknesses. Flight tests have been performed at two different sites. The first one was the QCAT Flight Test Area (about 180m×130m) in Brisbane. It contains several natural and man-made obstacles such as trees of various sizes, bushes, a microwave tower, fences, two sheds, two vehicles, and other small obstacles. The second site was the Burrandowan Flight Test Area (more than >200ha), which also contains a variety of obstacles and rough terrain with variant slope. It is important to note that all flight tests were performed without any a priori knowledge of the environment (terrain and obstacles) and all processing was done on board the helicopter.

TABLE I
TECHNICAL SPECIFICATIONS OF KEY SYSTEM COMPONENTS

Helicopter	12.3kg maximum takeoff weight
	1.78m rotor diameter
	23cm^3 two-stroke gasoline engine
	60min endurance
GNC system	L1 C/A GPS receiver (2.5m CEP), MEMS-based AHRS, high-res. barometric pressure sensor
	Hokuyo UTM-30LX 2D LIDAR with 270° field of view
	Vortex86DX 800MHz navigation computer
	Via Mark 800MHz flight computer
Inspection camera	12.1MP digital camera with 70° horizontal field of view

Table I contains technical specifications of the key components of our helicopter system. All computers run Linux with a real-time kernel patch and ESM[11]. All methods are implemented in ESM and C. Although the helicopter must execute an inspection task fully autonomously, our system

[11]ESM (*Extended State Machine*) is a software framework and state machine-based visual language developed for safety and time-critical robotic systems [18].

includes a ground station. We use the ground station for uploading flight plans, monitoring systems, setting system parameters, starting and aborting a mission, and terminating a flight. Furthermore, for technical reasons the ground station is required as a communication relay between the helicopter and the ADAC. Conceptually, however, a ground station is not required for task execution.

The different parameters used for terrain following and obstacle avoidance were mainly derived from the safe LIDAR range and the accuracy of state estimates and flight control. Their values have been refined based on flight experiments to provide the best tradeoff between the vehicle's safety (no collisions) and system performance (time to reach inspection points).

TABLE II

TERRAIN FOLLOWING AND OBSTACLE AVOIDANCE RESULTS

Method	Runs	Scenarios	Flight time
Terrain following	73	11	11.4h
Avoidance strategy 1	27	7	2.8h
Avoidance strategy 2	23	6	7.1h

Table II contains the flights we conducted for validating our approach. We had three situations where a backup pilot had to take over while testing within visual range and no failures during BVR flights. In the first situation the GPS failed (possibly caused by radio interference with the microwave tower at the QCAT site), in the second situation the control system could not cope with a strong wind gust while the helicopter was close to a tree, and in the third situation the helicopter was pushed towards the ground by a strong downdraft. In all three cases a critical design assumption was violated (see Section II). The risk of a failure during a BVR flight was decreased by increasing the safety distance to obstacles and by avoiding flights in doubtful weather and areas with GPS problems.

A. Terrain following

Terrain following experiments were conducted at both sites in different scenarios with closed-loop control. Initially, the terrain following system was tested alone without obstacle avoidance. In a second development stage, the complete system (terrain following and obstacle avoidance) was tested in different scenarios.

The first row of Table II shows the number of performed runs, the number of different scenarios, and the accumulated flight time. The helicopter followed in total more than 14km of terrain with a maximum tracking error of approximately 1m without ground collision or intervention by a backup pilot. However, in a few cases, the system aborted the mission and flew directly to the end point because the *heightMin* value fell below the safety threshold. It occurred when flying over complex terrain obstacles such as low roofs, fences and antenna poles at the QCAT site.

Figure 5 shows results of a terrain following flight at the QCAT flight test site. The helicopter was commanded to fly

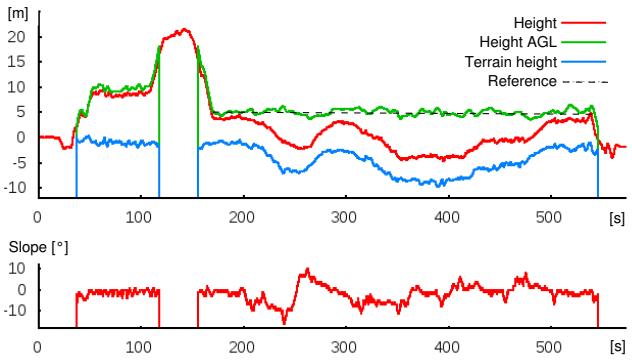

Fig. 5. Helicopter height and estimated terrain slope during a terrain following flight at 2m/s cruise speed and 5m height above ground.

to a series of waypoints, defining an obstacle-free flight path of about 450m around the compound. To stress the system we reduced the reference height to 5m and increased the cruise speed to 2m/s. The terrain height was estimated by subtracting the LIDAR-based height estimates (height above ground) from the pressure-based height estimates (height relative to take off point). During 370s of terrain following, the helicopter followed the terrain and maintained a 5m clearance from the ground with approximately 1m error in height regulation. As shown in the bottom of Figure 5, the slope computed by the perception system was also meaningful and close to the real terrain slope.

B. Obstacle avoidance and inspection missions

The second and third row of Table II summarize the results for obstacle avoidance strategy 1 and 2. All obstacle avoidance experiments included LIDAR-based terrain following and waggle cruise at 1m/s. The cruise speed for flights to and from an inspection area was set to 5m/s.

In these experiments, the waypoints are positioned such that there are obstacles between them. Therefore, if the helicopter attempts to fly a straight path between waypoints, it will collide with obstacles. Both strategies have been tested in a number of scenarios with different obstacle configurations including flights around single trees, groups of trees, sheds, etc.

Strategy 1 was tested at both the QCAT site as well as the Burrandowan site. Tests in Burrandowan included a BVR scenario which is described in Section IV-C. We have successfully completed[12] 10 missions for task 1 in seven different scenarios and 10 missions for task 2 in three different scenarios.

Strategy 2 was tested on the QCAT site which offers many challenging mission scenarios. We have successfully completed 12 missions for task 1 in six different scenarios and five missions for task 2 in three different scenarios. Figure 6 shows a successful tower inspection mission. This is a complex obstacle avoidance task as the tower is surrounded by a high metallic fence, several sheds, and trees of different

[12]Missions without image capture were considered successful if the helicopter reached correct image-capturing positions.

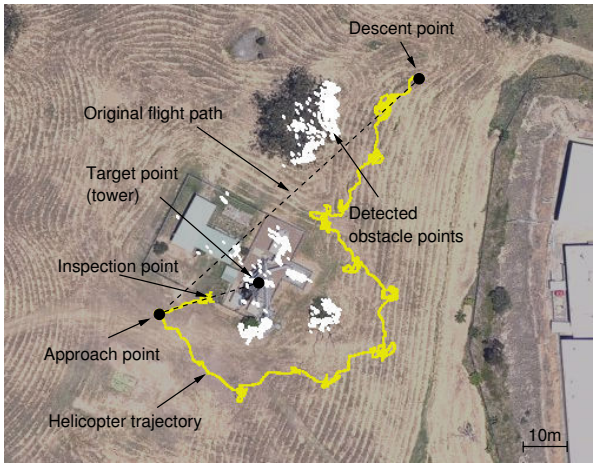

Fig. 6. Helicopter trajectory during a microwave tower inspection flight.

sizes. Moreover, the terrain is very uneven. Because of the safety distances, the helicopter did not find a path between the big tree in the north and the tower further south. This created a U-shaped obstacle configuration where reactive obstacle avoidance methods often fail. However, our approach succeeded and the helicopter flew to the approach point in the south-west.

The mission flight time for a flight in an obstacle free environment can be calculated based on distances, the regular cruise speed, the waggle cruise speed, and the vertical velocity. The extra time the helicopter needs to avoid obstacles depends on the number of avoidance waypoints it generates. The flight time per avoidance point is approximately one minute.

C. BVR windmill inspection

In December 2010, the final flight trials of the Smart Skies project took place at the Burrandowan flight test site. The objective of these tests was to demonstrate the integration of all components which have been developed in the project. The final demonstration flights involved several aircraft: (1) the CSIRO helicopter described in this paper; (2) an autonomous unmanned fixed-wing aircraft; (3) a manned light aircraft equipped with an autopilot for semi-autonomous flights; and (4) a number of simulated manned and unmanned aircraft.

In this paper, we describe the flight tests related to the CSIRO helicopter. The mission scenario consisted of a close inspection of a windmill (task 2 in Section II), located at about 1.4 km from the ground station. The geographic position of the windmill was provided with approximately 2.5m accuracy. The mission included three stages as explained in Section II.

We executed the BVR mission twice using strategy 1. Strategy 2 has been developed at a later stage. Both missions were successful. The wind speed at the ground station location was between 4 and 7m/s. Although the wind caused some worrying turbulences behind the trees in the inspection area, the mission execution was not affected.

Figure 7 shows the results of the first test where the helicopter was given the preference to turn right at the

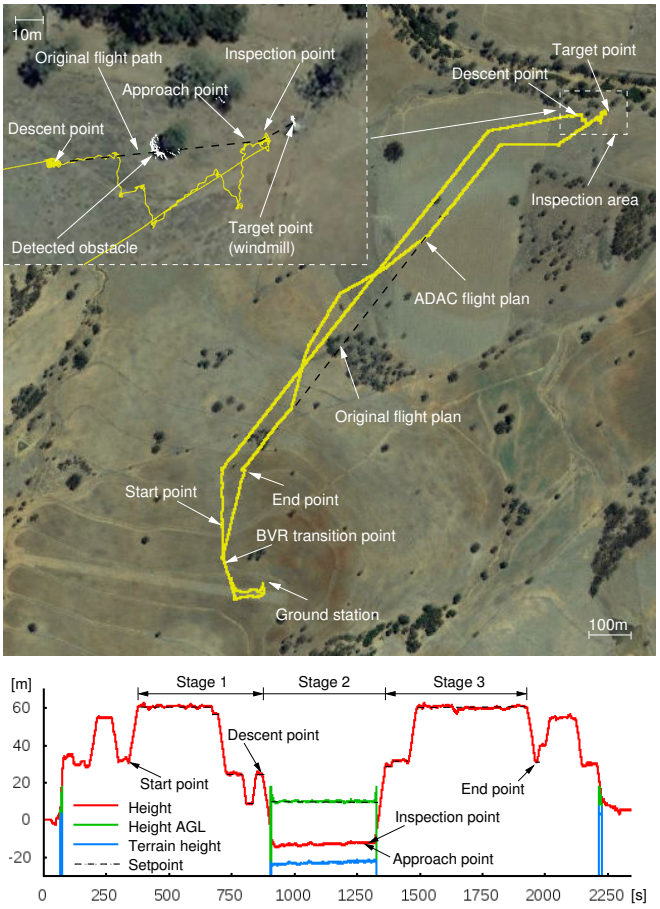

Fig. 7. Helicopter trajectory and height during the first BVR inspection flight.

first obstacle. The helicopter successfully flew BVR to the inspection area, regulated the height above ground to 10m, avoided obstacles and inspected the structure without user intervention[13]. During the mission no backup pilot was present in the inspection area. The last avoidance waypoint in the zoomed image was created due to a faulty implementation of the processing of very small LIDAR range readings when the helicopter is in obstacle free space. This problem has meanwhile been fixed. One can also see in Figure 7, that the helicopter received avoidance waypoints from the ADAC system during the way back in common airspace to avoid a collision with a simulated rotorcraft that was flying towards the helicopter. The helicopter successfully tracked the ADAC waypoints and avoided the simulated rotorcraft.

The second test was similar to the first one with the difference that this time we changed the preferred avoidance direction from right to left. We wanted to demonstrate the ability of the system to find its way to the approach point if there is no free path in the given direction.

Figure 9 shows the flight in the inspection area. It can be seen that the helicopter tried to avoid the obstacle from the left but after a certain number of attempts, it changed direction to avoid the obstacle from the right and reached

[13]For operational reasons, we uploaded separate flight plans for the three mission stages.

Fig. 8. Autonomous BVR inspection of a windmill: (a) the helicopter during the inspection; (b) inspection photo of the windmill taken by the helicopter from approximately 10m; (c) zoomed inspection photo.

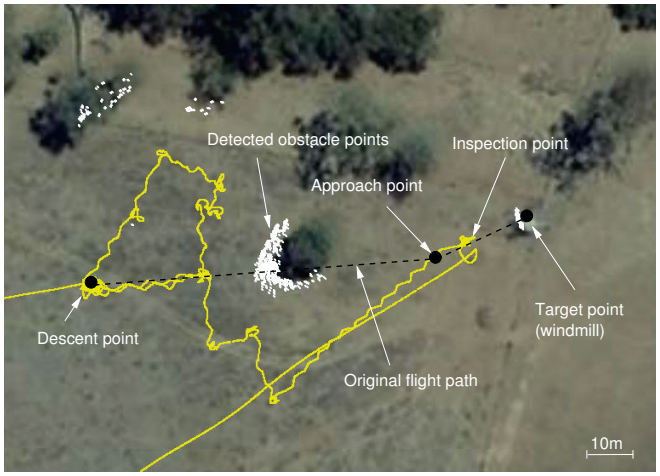

Fig. 9. Helicopter trajectory during the second BVR inspection flight.

the approach point. Figure 8 shows the helicopter during the inspection and and inspection photo of the windmill taken by the helicopter.

V. CONCLUSIONS

We presented a BVR obstacle avoidance and infrastructure inspection system implemented on an unmanned helicopter and flight tested in different mission scenarios. Although our approach is based on lightweight COTS sensors, simple perception methods and reactive behaviors, it provides a practical solution for flights close to ground and obstacles at modest speed. The speed during obstacle avoidance is mainly limited by the safe range of the LIDAR. The demonstrated capabilities have been proven to be sufficient to accomplish several real-world applications.

We proposed a method for terrain following and two strategies for goal-oriented obstacle avoidance. The second strategy includes heuristics to cope with a large variety of obstacle scenarios including concave shaped obstacle configurations. The helicopter is very likely to reach a destination if the size of an obstacle is within a specified limit and gaps are wide enough to pass through . The minimum gap width mainly depends on the width of the safety corridor of the helicopter. Our approach has not been designed for following narrow corridors often found in urban areas.

We recorded more than 11 hours of autonomous flight close to ground and obstacles in unknown environments with very few failures. We also demonstrated two BVR inspection flights without a backup pilot. The proposed methods are suitable for implementation on any robotic helicopter with a vertically mounted 2D scanning LIDAR and can be integrated with any waypoint based path planner.

VI. ACKNOWLEDGMENTS

This research is part of the Smart Skies Project and is supported, in part, by the Queensland State Government Smart State Funding Scheme. The authors gratefully acknowledge the contribution of the Smart Skies partners and all CSIRO UAS team members. In particular we would like to thank Brett Wood for the technical support and Bilal Arain for improving the attitude control of the helicopter.

REFERENCES

[1] B. Herisse, T. Hamel, R. E. Mahony, and F. X. Russotto, "A terrain-following control approach for a VTOL unmanned aerial vehicle using average optical flow," *Autonomous Robots*, vol. 29, no. 3-4, pp. 381–399, 2010.

[2] F. Ruffier and N. Franceschini, "Optic flow regulation: the key to aircraft automatic guidance," *Elsevier, Robotics and Autonomous Systems*, no. 50, pp. 177–194, 2005.

[3] M. A. Garratt and J. S. Chahl, "Vision-based terrain following for an unmanned rotorcraft," *Journal of Field Robotics*, vol. 25, no. 4-5, pp. 284–301, 2008.

[4] J.-C. Zufferey and D. Floreano, "Fly-inspired visual steering of an ultralight indoor aircraft," *IEEE Transactions On Robotics*, vol. 22, no. 1, pp. 137–146, 2006.

[5] B. William, E. Green, and P. Oh, "Optic-flow-based collision avoidance," *IEEE Robotics and Automation Magazine*, pp. 96–103, March 2008.

[6] S. Hrabar and G. S.Sukhatme, "Vision-based navigation through urban canyons," *Journal of Field Robotics*, vol. 26, no. 5, pp. 431–452, 2009.

[7] A. Beyeler, J.-C. Zufferey, and D. Floreano, "Vision-based control of near-obstacle flight," *Autonomous Robots*, vol. 27, pp. 201–219, 2009.

[8] J. Conroy, G. Gremillion, B. Ranganathan, and J. S. Humbert, "Implementation of wide-field integration of optic flow for autonomous quadrotor navigation," *Autonomous Robots*, vol. 27, pp. 189–198, 2009.

[9] F. Andert, F.-M. Adolf, L. Goormann, and J. S. Dittrich, "Autonomous vision-based helicopter flights through obstacle gates," *Journal of Intelligent and Robotic Systems*, vol. 57, no. 1-4, pp. 259–280, Jan. 2010.

[10] F. Andert and F. Adolf, "Online world modeling and path planning for an unmanned helicopter," *Autonomous Robots*, vol. 27, pp. 147–164, 2009.

[11] J. Byrne, M. Cosgrove, and R. Mehra, "Stereo based obstacle detection for an unmanned air vehicle," in *Proceedings of the IEEE International Conference on Robotics and Automation, ICRA 2006*, Orlando, USA, May 2006, pp. 2830–2835.

[12] S. Scherer, S.Singh, L. Chamberlain, and M. Elgersma, "Flying fast and low among obstacles: Methodology and experiments," *International Journal of Robotics Research*, vol. 27, no. 5, pp. 549–574, May 2008.

[13] P. Tsenkov, J. K. Howlett, M. Whalley, G. Schulein, M. Takahashi, M. H. Rhinehart, and B. Mettler, "A system for 3D autonomous rotorcraft navigation in urban environments," in *Proceedings of the AIAA, AIAA-2008-7412*, San Diego, USA, Sept. 2008.

[14] M. Whalley, M. Takahashi, P. Tsenkov, and G. Schulein, "Field-testing of a helicopter UAV obstacle field navigation and landing system," in *Proceedings of the 65th Annual forum of the American Helicopter Society (AHS)*, Grapevine, USA, May 2009.

[15] D. H. Shim, H. Chung, and S. Sastry, "Conflict-free navigation in unknown urban environments," *IEEE Robotics and Automation Magazine*, vol. 13, pp. 27–33, Sept. 2006.

[16] A. Bachrach, R. He, and N. Roy, "Autonomous flight in unknown indoor environments," *International Journal of Micro Air Vehicles*, vol. 1, no. 4, pp. 217–228, 2009.

[17] R. Clothier, R. Baumeister, M. Brünig, A. Duggan, and M. Wilson, "The Smart Skies project," *IEEE Aerospace and Electronic Systems Magazine*, vol. 26, no. 6, pp. 14–23, June 2011.

[18] T. Merz, P. Rudol, and M. Wzorek, "Control system framework for autonomous robots based on extended state machines," in *International Conference on Autonomic and Autonomous Systems, ICAS'06*, Silicon Valley, USA, July 2006.